International Journal for Innovative Engineering and Management Research
PEER REVIEWED OPEN ACCESS INTERNATIONAL JOURNAL
www.ijiemr.org

MICROSTRUCTURAL EVOLUTION AND PERFORMANCE ASSESSMENT OF GRADE V TITANIUM ALLOY

VIVEK KUMAR,
JOINT DIRECTOR, LABOUR RESOURCES DEPARTMENT, GOVT. OF BIHAR

ABSTRACT

The development and performance of the microstructure of α+β Ti-6Al-4V alloy when it is heated under controlled conditions are examined in this work. The alloy was heated to 955°C in a tube furnace to produce a full β-phase transition. It was then cooled either by air or water quenching. The alloy was obtained in plate form according to AMS 4911L requirements. Two, three, and four hours of aging treatments improved mechanical characteristics. Analyzing the α and β platelet structures was done using optical microscopy. This study shows that the microstructure and, by extension, the performance of Ti-6Al-4V alloy are very sensitive to the heat treatment conditions.

Keywords: Microstructural, Thermo mechanical Processing, Mechanical Properties, Corrosion Resistance.

INTRODUCTION

Titanium and its alloys are crucial engineering materials in state-of-the-art technological applications due to their exceptional biocompatibility, high strength-to-weight ratio, and superior corrosion resistance. An essential kind of titanium alloy is grade V, sometimes called Ti-6Al-4V. This alloy accounts for about half of the world's titanium use; its primary constituents are vanadium (around 4% of the total) and aluminum (approximately 6%). Many industries, such as chemical processing, biomedicine, the maritime industry, and aerospace, need high performance under severe service conditions. In these domains, it is extensively used. The remarkable performance of Ti-6Al-4V is largely attributable to its malleable microstructure, which allows it to undergo thermomechanical processing to get specific mechanical and physical properties. It is important to comprehend the microstructural evolution throughout various processing steps in order to maximize the performance of this alloy for specific uses. The two separate phases that make up the nanostructure of Ti-6Al-4V are beta (β) and alpha (α). Alpha phase hexagonal close-packed (HCP) structure provides better creep resistance and strength at elevated temperatures, while beta phase body-centered cubic (BCC) structure enhances workability and toughness. The distribution, form, and proportion of these phases may be changed using heat treatments and mechanical working methods including rolling, additive manufacturing, and forging. Microstructural management has a direct influence on critical material properties such as ductility, hardness, fatigue life, tensile strength, and resistance to wear and corrosion. The successful use of Ti-6Al-4V in high-performance applications is dependent on the exact measurement and monitoring of microstructural changes.

Grade V titanium alloy microstructural development is heavily influenced by the processing conditions, including temperature history and deformation. A completely beta microstructure results from processing above the beta transus temperature; when cooled, it may assume several alpha morphologies, including equiaxed, lamellar, or martensitic structures, according on the pace of cooling. In contrast, sub-transus processing encourages the presence of small alpha grains scattered across a beta matrix while preserving the two-phase microstructure. The variations in microstructure have a significant effect on mechanical performance. While a lamellar alpha structure increases strength at the expense of fracture toughness, a fine equiaxed alpha structure improves fatigue resistance and ductility. To achieve application-specific performance in Ti-6Al-4V alloys, it is crucial to precisely regulate processing parameters in order to tune the microstructure. Additive manufacturing (AM) has recently emerged as a viable option for producing intricate Ti-6Al-4V parts with tailored microstructures, thanks to processes like selective laser melting (SLM) and electron beam melting (EBM). The distinctive microstructural characteristics, such columnar grain development and acicular alpha martensite, are produced by the fast solidification rates and thermal cycling introduced by these layer-by-layer production processes. A post-processing heat treatment may be necessary to optimize properties due to residual stresses and anisotropy introduced by these characteristics, even if they may increase strength. Therefore, in order to comprehend the as-built characteristics and to develop efficient post-processing methods, precise microstructural characterisation is crucial.

LITERATURE REVIEW

Campanella, Davide et al., (2022) the aerospace sector has recently begun to favor titanium and titanium alloys, particularly the high-strength Titanium Grade5, when it comes to metal components. Forming operations on Titanium Grade 5 need high temperatures due to the material's low formability at ambient temperature. The formability and product quality are greatly affected by the particular microstructure that develops under these circumstances as a consequence of the heating and deformation cycles. However, additive manufacturing technologies like electron beam melting and selective laser melting are displacing more conventional methods like machining and forging. The manufacturing technique is crucial in determining the mechanical and microstructural qualities, geometric precision, surface quality, and other fundamental component attributes. In order to help readers choose the best manufacturing route for their specific application and part design, the authors of this paper set out to compare and contrast various manufacturing alternatives for aeronautical parts, taking into account their inherent characteristics.

Fatoba, Olawale et al., (2020) Surface modification has the potential to enhance the surface integrity of titanium alloy, making it more versatile and applicable to a wider range of industrial uses. The advent of additive manufacturing has the potential to revolutionize how we see design and fabrication, and it is also a very competitive production approach from a business perspective. This research looks at the microstructure of Ti-6Al-4V grade 5 alloy as a consequence of varying the Ytterbium Laser System's process parameters, including laser power, powder feed rate, and traverse speed. The Ytterbium Laser System (YLS-2000-TR), a 3kW (CW) unit, was used to deposit the material on top of the reinforcing powder. Scanning laser power and speed were adjusted between 900 and 1000 W, with the former ranging from 1 to 1.2 m/min. The gas flow rate, spot diameter, and powder flow rate were the only other variables held constant. Scanning electron microscopy (SEM) and optical microscopy (OM) were used to describe the microstructure by morphology and grain size. The formation of the transformed α+H microstructure from the initial primary α microstructure, the development and evolution of unique grain morphologies, and the stability of the alpha and beta structures upon increased and reduced structures were all effects of the thermal histories induced by the DLMD process. It was found that the breadth of the columnar grains was reduced as a consequence of faster cooling rates, which were brought about by faster traversal speeds.

Zhao, Zhiyong et al., (2020) we prepared the ultra-fine-grained Ti-6Al-4V alloy using multipass ECAP. In this work, we looked at how the mechanical properties and microstructure of Ti-6Al-4V alloy changed throughout the ECAP process. There were a lot of grains in the four-pass ECAP sample that were 200-300 nm in size, and the grain size of the Ti-6Al-4V alloy dramatically dropped as the number of ECAP passes increased. During the multipass ECAP process, the twins steadily increase in number, reflecting the critical function of the twinning structure in the plastic deformation coordination mechanism. Vickers hardness and room-temperature compression strength also rose as ECAP pass counts raised a result of the high dislocation density, grain refinement, and many twins. Hardness rose to 392 HV and compression strength to 1432 MPa, from 355 HV and 1296 MPa, respectively. With its highly twinning density and consistently refined microstructure, the four-pass ECAP sample achieves a final strain that surpasses that of the two-pass and three-pass samples considerably. By using four-pass ECAP and then annealing the material at 923 K for 30 minutes, a uniform microstructure was achieved with an average grain size of 1-2 μm. This suggests that static recrystallization happens at a low temperature and in a short amount of time. According to the findings of the compression tests, the Ti-6Al-4V alloy that was made using four-pass ECAP and then subjected to annealing has excellent plasticity and strength at room temperature, with ultimate strain values of 48.8% and strength values of 1400.3 MPa, respectively.

Bodunrin, Michael et al., (2019) this research examined the changes in microstructure that took place throughout the hot forming process of Ti-6Al-4V, which started with elongated and equiaxed hcp α grains and a web of intergranular bcc β-phase. Various strain rates (0.01, 1, and $10 s^{-1}$) and deformation temperatures (800-950 °C) were tested in isothermal compression experiments utilizing the Gleeble 3500 thermomechanical simulator. Optical and scanning electron microscopy was used to analyze the microstructures of the distorted

International Journal for Innovative Engineering and Management Research
PEER REVIEWED OPEN ACCESS INTERNATIONAL JOURNAL
www.ijiemr.org

samples. The photos were examined with the help of ImageJ 1.48V. Known processes that regulate the deformation behavior of titanium alloys, dynamic globularization and dynamic recovery, were shown to have a significant impact on the alloy's hot forming. Under certain deformation circumstances, however, Ti-6Al-4V with a complicated beginning microstructure exhibited unusual phenomena, such as deformation-induced phase change and aberrant grain development, which are not often seen in Ti-6Al-4V alloys with standard starting microstructures. When the strain rates were greater (1 and 10 s^{-1}) and the deformation temperatures were lower, abnormal grain development started. The alloy's β transus temperature was lowered by 45 °C at a modest strain rate of 0.01 s^{-1} due to deformation-induced phase transition.

XU, Sheng-hang et al., (2018) Using a constant temperature gradient between 600 and 700 °C, a novel high throughput heat-treatment process was used to the Ti-5553 alloy (Ti-5Al-5Mo-5V-3Cr, mass fraction, %). The direct current heated the sample's axial section, which caused it to vary, thereby inducing the temperature gradient. Using the end quenching approach, the treated sample might experience a range of continuous cooling speeds. We looked at how the microstructure changed and the mechanical characteristics changed under various heat treatment settings. The alloy undergoes pseudo-spinodal breakdown at (617±1) °C, and the precipitated α phase has a size of around 300 nm, according to the data. In addition, the pseudo-spinodal decomposition temperature is maintained for 4 hours throughout the heat treatment to achieve the maximum microhardness. These results show that the high throughput approach can quickly and efficiently find the alloys' phase transition temperatures and the related changes in their microstructure.

Wu, Songquan et al., (2016) Optical microscopy, scanning electron microscopy, transmission electron microscopy, and the Vickers hardness tester were used to systematically examine the microstructure and hardness of a powder-bed-type selective laser melted Ti-6Al-4V alloy following post heat treatments at temperatures ranging from 300 °C to 1020 °C. In the specimen that was obtained, many features were observed, including long columnar original β grains, a checkerboard pattern in the top view, and inside dominated parallel acicular martensite in the side view. The original columnar β grain cannot be changed in shape by subtransus heat treatment; instead, it decomposes into α platelets and either the surrounded β phase or the transformed α' phase, depending on the heating temperature. In contrast, the original long columnar β grain would be completely broken up by supertransus heat treatment, leaving only the large original equiaxial β grain filled with the newly formed weave-type acicular α' martensite, just like the wrought specimen that underwent supertransus heat treatment. At approximately 500 °C, there is a substructural refinement effect; at around 1000 °C, there is a martensitic refinement effect; and at around 875 °C, there is a softening effect due to the complete decomposition of the martensite. The hardness-temperature plot shows a double peak phenomenon, which is explained by the microstructural change trend.

International Journal for Innovative Engineering and Management Research
PEER REVIEWED OPEN ACCESS INTERNATIONAL JOURNAL
www.ijiemr.org

Hadke, Shreyash et al., (2015) the impact of ageing and quenching on the microstructure and abrasive wear of Ti-6Al-4V alloy is examined in this research. Ageing at 823 K for 4 hours (14,400 s) followed solution treatment at 1339 K and oil quenching of the as-received alloy. Optical microscopy, scanning electron microscopy, energy dispersive spectroscopy, and electron backscattered diffraction were used to analyze the microstructures of the specimens both as-received and quench-aged. The specimen that was obtained had α grain that was very fine, with an average grain size of 2 μm, and β phase that was evenly distributed throughout. The microstructure of the specimen that was aged in a quench revealed α plate, which was created when α′ decomposed throughout the aging process. During the aging process, the β phase separated from the α′ martensite and was therefore evenly distributed throughout the α matrix. With the hope that its enhanced hardness would improve its resistance to abrasive wear, the Ti-6Al-4V alloy was quench-aged to its maximum hardness. The specimens were subjected to two-body abrasive wear tests utilizing pin-on-disk equipment and SiC abrasive medium (150-grit size) after being quench-aged and as received. Researchers looked at how abrasive wear behaved under different sliding distance and standard load conditions. The quench-aged specimen had higher wear resistance and harder material than the as-received specimen; however the reverse was not true. The morphology/microstructure of the alloy and the accompanying wear mechanism(s) have been used to explain the abrasive wear behavior of Ti-6Al-4V alloy.

MATERIAL AND METHODS

- **Materials used**

The α+β Ti-6Al-4V alloy, which was obtained in plate form and met the requirements stated in AMS 4911L, was the substance that was examined. Table 1 displays the chemical make-up of the raw material.

Table 1: Chemical composition of as-received Ti-6Al-4V alloy in wt. %

Element	Concentration (wt.%)
Aluminum	6.75
Vanadium	4.50
Iron	0.30
Oxygen	0.20
Carbon	0.08
Nitrogen	0.05

Hydrogen	0.015
Yttrium	0.005
Titanium	Balance

- **Heat Treatment**

Ti64, the titanium alloy, was heat treated in a very controlled environment. The use of a tube furnace allowed for the careful control of the heating process, which prevented any unwanted oxidation. From a beginning temperature of 25°C and increasing to a final temperature of 955°C, which represents a single-phase β region in the alloy's phase diagram, the material was heated at a rate of 10°C per second. The microstructure was allowed to fully change into the desired β phase by holding it for one hour after it reached this critical temperature.

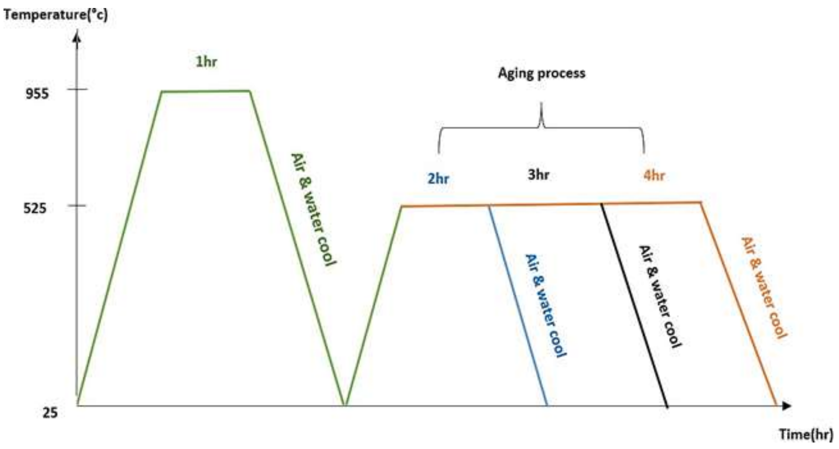

Fig. 1: Solution heat treatments and aging treatments of Ti-6Al-4V.

Afterwards, the specimens were chilled; some were cooled in air and others were quickly cooled in water. After this heat treatment step, the samples were cooled and then subjected to an aging method to increase their mechanical strength. Specimens aged for 2, 3, and 4 hours, respectively, during this procedure. It should be mentioned that the aging process made use of both air-cooling and water-quenching approaches. Figure 1 shows the whole heat treatment process, including the microstructural changes and improved properties that come from it.

Characterization

We prepared the samples according to standard AMS 4911L to ensure proper characterization. The microstructural features, α and β platelet structure, and optical microscopy were studied.

RESULTS AND DISCUSSION

- **Microstructure**

Figure 2 shows the results of an optical microscope analysis of the grain distribution. The existence of phases inside the microstructure was determined by capturing the pictures at a lower magnification level. The aging process led to the attainment of Fig. 2b to 2f. The initial state has a balanced structure with a higher number of α phases compared to β phases. This is because the elementary matrix has a high concentration of Al and V. Grain borders are clearly evident, and grains themselves are clearly visible.

Figures 2b and 2c show minor alterations in microstructure, indicating that both are beginning to form β phases rather than α phases. The gradual cooling of the material during annealing causes the nucleation of β, which can be seen in Fig. 2b. The structure contains the protuberance of the alpha phase. Figure 2c, on the other hand, shows a bi-modal microstructure, which is consistent with what Dewangan and Singhal found. Figures 2e and 2f show that the β phases are now more prevalent in water-quenched samples compared to air-cooled samples as the aging duration rises.

The fact that the α phases exhibit non-uniformity and reveal that the secondary α phases have varying particle sizes is also important to mention. After quenching the β phase in water, the aging temperature, which is somewhat lower than the β temperature, allows for the achievement of the maximum amount of α'. After the 550°C aging treatment, significant microstructure changes were seen. More specifically, the microstructure showed smaller islands that corresponded to the major α phase. A unique and intricate microstructural arrangement was formed when these islands lived in harmony with colonies of thin α and β plates. This change causes a substantial alteration to the material's structure and composition, which in turn affects its mechanical characteristics and behavior. The loss of β phases in the microstructure increases with increasing age time (especially with water-quenched samples), as seen in Fig. 2. This leads to a stronger alloy with less ductility.

International Journal for Innovative Engineering and Management Research
PEER REVIEWED OPEN ACCESS INTERNATIONAL JOURNAL
www.ijiemr.org

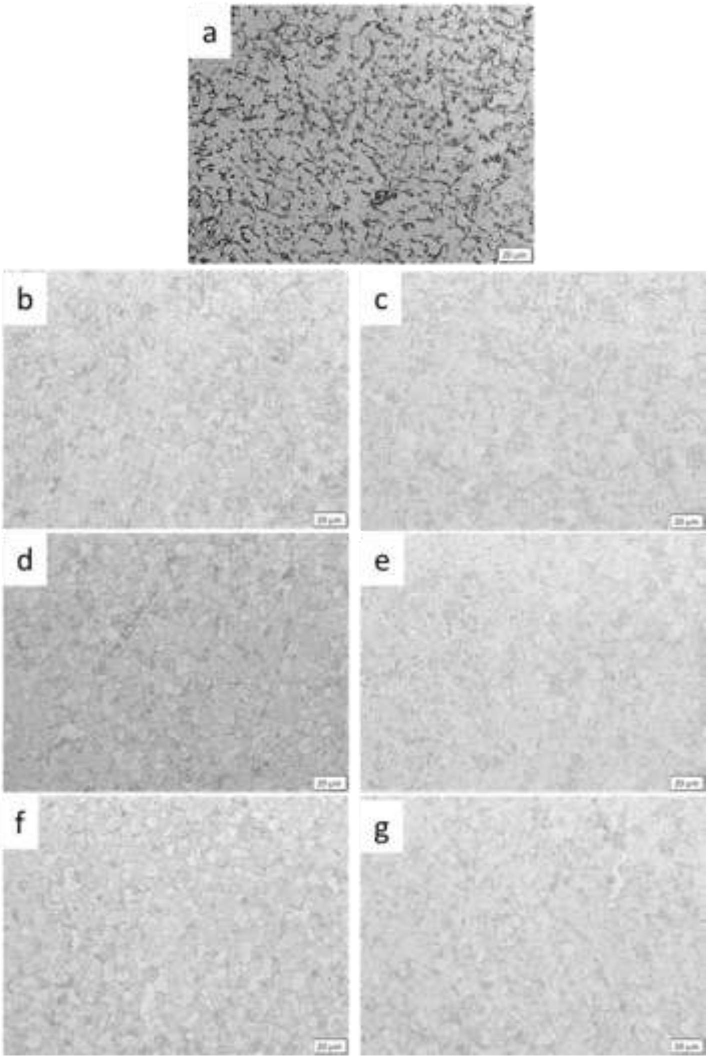

Figure 2: Microstructures of: a) As-received Ti64, b) AC-2hrs, c) WQ-2hrs, d) AC-3hrs, e) WQ-3hrs, f) AC-4hrs, and g) WQ-4hrs, respectively

3.2 MECHANICAL PROPERTIES

- **Hardness**

The hardness values of Ti64 are compared in Figure 3. A strong relationship between the amount of time water-quenched materials spend aging and the disappearance of unstable β phases is shown by the findings.

International Journal for Innovative Engineering and Management Research
PEER REVIEWED OPEN ACCESS INTERNATIONAL JOURNAL
www.ijiemr.org

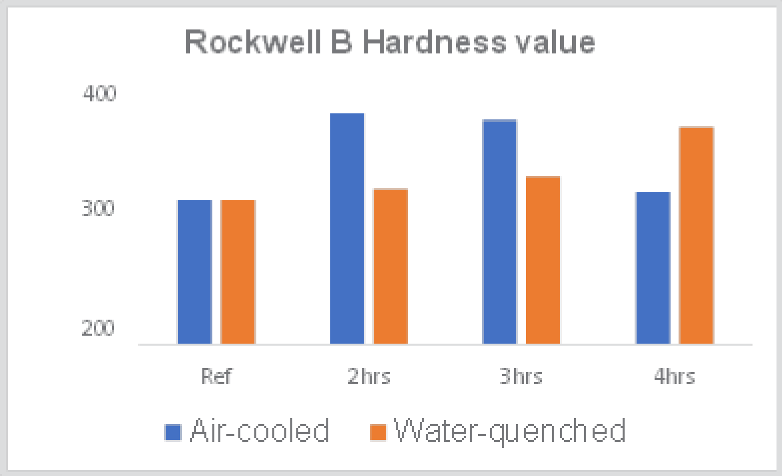

Figure 3: Hardness values of Ti-6Al-4V.

There is a noticeable decrease in the presence of these unstable β phases as the aging time increases. An enhanced hardness characteristic was seen in the sample that was aged for 4 hours. When looking at samples that have been cooled by air, on the other hand, hardness levels tend to drop as the aging period increases. When compared to the reference sample, the sample that was added for 2 hours showed a 150 HRB increase in hardness value, but this value decreased with time. The hardness testing results showed that the water-quenched samples were harder as the treatment intensity rose. This suggests that microstructural modifications had an impact. Notably, our results are supported by Yaser et al., who have also documented a similar pattern in the hardness levels of water-quenched samples. As the treatment continued, the link between microstructure, strength, and ductility was highlighted by an increase in ultimate tensile strength and a commensurate decrease in elongation. The reason for this is the ductile and somewhat soft unstable β phase.

- **Wear resistance**

When it comes to materials that are exposed to sliding contacts, wear is an important factor to consider in many engineering applications. Improving material performance and component durability requires a thorough understanding of wear behavior, particularly in titanium. In order to determine wear trends and understand the causes of wear resistance, we used Equations 1–3 to examine the wear characteristics of titanium samples under different situations.

$$\text{Wear Volume} = \frac{\pi h}{6}\left[\frac{3}{4}d^2 + h^2\right] \tag{1}$$

$$\text{Wear Rate} = \frac{Wear\ Volume}{Sliding\ Volume} \tag{2}$$

$$\text{Wear Resistance} = \frac{1}{Wear\ Rate} \tag{3}$$

Where d denotes the average width of the worn scar and h stands for the average heights of the depression. The tribometer yielded these results. Figure 4 shows a micrograph of the wear mechanism.

Table 2: The wear characteristics obtained and calculated from the tribometer output

Sample	dh (µm)	dx (µm)	Sliding Distance (m)	Wear Volume (mm^3)	Wear Rate (mm^3/m)	Wear resistance (m/mm^3)
Ref	0.578	335.23	0.00182	2.55E-05	0.01400	071.4086
AC2	0.230	227.16	0.00163	4.66E-06	0.00286	349.6791
WQ2	0.884	296.72	0.00162	3.06E-05	0.01887	052.9976
AC3	1.346	354.94	0.00169	6.66E-05	0.03941	025.3758
WQ3	0.180	243.25	0.00157	4.18E-06	0.00266	375.3351
AC4	0.311	279.82	0.00168	9.55E-06	0.00568	175.9479
WQ4	0.433	237.56	0.00156	9.59E-06	0.00615	162.7289

Titanium sample wear characteristics in different environments may be better understood with the help of the collected data. Indicators of material loss due to wear may be found in these wear volume metrics. The samples AC2 and WQ3, in particular, stand out with the lowest wear volumes, indicating substantially increased wear resistance; these samples outperform the others by 80% and 83%, respectively. Wear volumes are somewhat larger in samples WQ3 and AC3, suggesting that they are more prone to material loss. Still, these wear volumes are much lower than those of untreated Ti64.

How much material is being removed over the sliding distance may be learned from the wear rates. The samples AC2 and WQ3 showed the least amount of wear, which means they are very resistant to wear. It is worth noting that samples AC3 and WQ4 had greater wear rates compared to their lower wear volumes. This suggests that these samples may have experienced distinct types of wear, maybe due to the wider wear track. A material's wear resistance under a given set of circumstances is shown by the wear resistance parameter, which is the inverse of the wear rate. Sample WQ3 outperformed the others in the sliding circumstances by displaying the maximum wear resistance. Figure 4 shows the wear profile, which shows the patterns in wear for both the untreated and treated TI-6Al-4V. Ploughing activity in the counter face due to hard asperities was seen in Reference, AC3, and WQ2 throughout the study.

International Journal for Innovative Engineering and Management Research
PEER REVIEWED OPEN ACCESS INTERNATIONAL JOURNAL
www.ijiemr.org

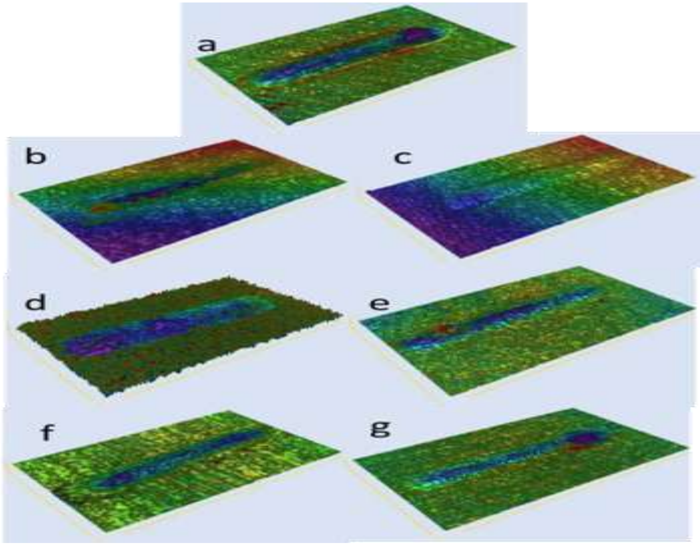

Figure 4: Wear profile of: a) As-received Ti64, b) AC-2hrs, c) WQ-2hrs, d) AC-3hrs, e) WQ-3hrs, f) AC- 4hrs, and g) WQ-4hrs, respectively

This suggests that the samples underwent significant plastic deformation as a result of the high amount of wear shown in the deeper grooves. In other cases of heat treatment, an adhesive wear mechanism is seen. With the exception of wear rate, all other characterizations exhibit a clear pattern.

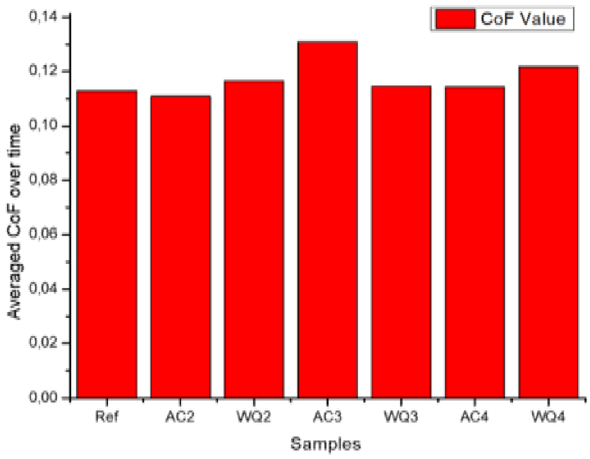

Figure 5: Averaged coefficient of friction of the samples under different conditions

In dry sliding circumstances, the coefficient of friction was studied with a standard load of 5 kgf. In Figure 5, we can see the mean values. There is no clear pattern in these values throughout the wear profile data. This point to the existence of many processes and regions of yielding contact, which cause the frictional forces to be unevenly distributed along and across the worn track junctions.

CONCLUSION

Grade V titanium alloy (Ti-6Al-4V) microstructural development and performance evaluation research demonstrates the important link between processing parameters, microstructure, and material efficiency. The mechanical strength, ductility, fatigue resistance, and corrosion behavior of the alloy can be altered by changing its microstructure, specifically the distribution and shape of its alpha and beta phases. This was discovered through a combination of thermo mechanical treatments and sophisticated characterization methods. The optimization of microstructure for individual application needs is made possible by tailored processing approaches, which include both traditional and additive manufacturing processes. Grade V titanium components used in aerospace, biomedical, and industrial applications must have exact control over microstructural characteristics to improve reliability and efficiency, according to the results.

REFERENCES:

[1] O. Fatoba, S. Akinlabi, E. Akinlabi, L. Naidoo, A. Adediran, and O. Odebiyi, "Microstructural enhancement and performance of additive manufactured titanium alloy grade 5 composite coatings," in *Proc. Int. Mech. Eng. Congr. Expo.*, 2020, pp. 1–12.

[2] Z. Zhao, G. Wang, Y. Zhang, J. Gao, and H. Hou, "Microstructure evolution and mechanical properties of Ti-6Al-4V alloy prepared by multipass equal channel angular pressing," *J. Mater. Eng. Perform.*, vol. 29, no. 1–2, 2020.

[3] M. Bodunrin, L. Chown, J. van der Merwe, and K. Alaneme, "Microstructural evolution during hot forming of Ti-6Al-4V alloy with complex initial microstructure," *Int. J. Adv. Manuf. Technol.*, vol. 104, no. 2, 2019.

[4] S. XU, Y. Liu, B. Liu, X. Wang, and Z. CHEN, "Microstructural evolution and mechanical properties of Ti–5Al–5Mo–5V–3Cr alloy by heat treatment with continuous temperature gradient," *Trans. Nonferrous Met. Soc. China*, vol. 28, no. 2, pp. 273–281, 2018.

[5] B. Tang, H. Kou, X. Zhang, P. Gao, and J. Li, "Study on the formation mechanism of α lamellae in a near β titanium alloy," *Prog. Nat. Sci.: Mater. Int.*, vol. 26, pp. 385–390, 2016.

[6] S. Wu et al., "Microstructural evolution and microhardness of a selective-laser-melted Ti-6Al-4V alloy after post heat treatments," *J. Alloys Compd.*, vol. 672, 2016.

[7] L. Li, J. Luo, J. J. Yan, and M. Q. Li, "Dynamic globularization and restoration mechanism of Ti–5Al–2Sn–2Zr–4Mo–4Cr alloy during isothermal compression," *J. Alloys Compd.*, vol. 622, pp. 174–183, 2015.

[8] S. Hadke, R. Khatirkar, S. K. Shekhawat, S. Jain, and S. Sapate, "Microstructure evolution and abrasive wear behavior of Ti-6Al-4V alloy," *J. Mater. Eng. Perform.*, vol. 24, no. 10, 2015.

[9] J. K. Fan, H. C. Kou, M. J. Lai, B. Tang, H. Chang, and J. S. Li, "Hot deformation mechanism and microstructure evolution of a new near-β titanium alloy," *Mater. Sci. Eng. A*, vol. 584, pp. 121–132, 2013.

[10] Y. C. Zhu, W. D. Zeng, J. L. Liu, Y. Q. Zhao, Y. G. Zhou, and H. Q. Yu, "Effect of processing parameters on the hot deformation behavior of as-cast TC21 titanium alloy," *Mater. Des.*, vol. 33, pp. 264–272, 2012.

[11] W. Jia, W. Zeng, Y. Han, J. Liu, Y. Zhou, and Q. Wang, "Prediction of flow stress in isothermal compression of Ti60 alloy using an adaptive network-based fuzzy inference system," *Mater. Des.*, vol. 32, no. 10, pp. 4676–4683, 2011.

[12] Y. C. Lin and G. Liu, "A new mathematical model for predicting flow stress of typical high-strength alloy steel at elevated high temperature," *Comput. Mater. Sci.*, vol. 48, no. 1, pp. 54–58, 2010.

[13] J.-K. Chang, K. Takata, K. Ichitani, and E. M. Taleff, "Abnormal grain growth and recrystallization in Al-Mg alloy AA5182 following hot deformation," *Metall. Mater. Trans. A*, vol. 41, no. 8, pp. 1942–195, 2010.

[14] L. J. Huang, G. Geng, A. B. Li, X. P. Cui, H. Z. Li, and G. S. Wang, "Characteristics of hot compression behavior of Ti–6.5Al–3.5Mo–1.5Zr–0.3Si alloy with an equiaxed microstructure," *Mater. Sci. Eng. A*, vol. 505, no. 1–2, pp. 136–143, 2009.

[15] P. Wanjara, M. Jahazi, H. Monajati, S. Yue, and J.-P. Immarigeon, "Hot working behavior of near-α alloy IMI834," *Mater. Sci. Eng. A*, vol. 396, no. 1–2, pp. 50–60, 2005.

[16] R. Ding, Z. X. Guo, and A. Wilson, "Microstructural evolution of a Ti–6Al–4V alloy during thermo mechanical processing," *Mater. Sci. Eng. A*, vol. 327, no. 2, pp. 233–245, 2002.